

TECHNICAL DEVELOPMENT REPORT NO. 262

EVALUATION OF THE  
FTL-21A VOR SPINNING ANTENNA

FOR LIMITED DISTRIBUTION

by

Samuel E. Taggart  
Thomas S. Wonnell  
Walter M. Ehler

Electronics Division

February 1955

CIVIL AERONAUTICS ADMINISTRATION  
TECHNICAL DEVELOPMENT  
AND EVALUATION CENTER  
INDIANAPOLIS, INDIANA

## EVALUATION OF THE FTL SPINNING VOR ANTENNA

### SUMMARY

This report gives an evaluation of a production model of the FTL-21A VOR spinning antenna developed by the Federal Telecommunication Laboratories, Inc. Ground and flight tests which were conducted are described. The bearing and polarization errors were acceptable, although the array was found to be somewhat sensitive to phasing adjustment. The distance range and stability of the system were comparable to the four-loop VOR array. The method suggested by the manufacturer for phasing the array may be improved upon if means are provided for measurement of bearing error at the edge of the counterpoise. In designing the array, the manufacturer considered ease of installation and maintenance by personnel with limited training. These objectives appear to have been adequately met.

### INTRODUCTION

The evaluation tests described in this report were conducted early in 1954 at the Technical Development and Evaluation Center, Indianapolis, Indiana, and are supplemental to tests conducted on an earlier model of the antenna<sup>1</sup>. The tests were (1) to determine what improvements had been made in the newer production model of the spinning type VOR antenna, (2) to compare its performance with that of a CAA standard four-loop VOR antenna, and (3) to test the feasibility of making bearing calibration tests of such an antenna at the edge of the counterpoise<sup>2</sup>.

The spinning antenna was tested on a circular counterpoise 35 feet in diameter and 10 feet high. The counterpoise was made of solid pieces of galvanized sheet metal soldered along all joints. Most of the bearing calibration tests were conducted at the edge of the counterpoise in the manner described in an earlier report<sup>3</sup>. Two types of monitors were used in making the bearing error check at the edge of the counterpoise and additional measurements of bearing errors were made at the receiver laboratory located at a distance of 3,725 feet. Data for error curves were also obtained at the edge of the counterpoise and at the receiver laboratory simultaneously while rotating the entire antenna array.

<sup>1</sup> Thomas S. Wonnell, "Evaluation of Federal Telecommunications Laboratories Omnirange Antenna," CAA TD Report No. 111, May 1950.

<sup>2</sup> Robert B. Flint and William L. Wright, "Ground Calibration of the VOR," CAA TD Report No. 227, January 1954.

<sup>3</sup> Ibid.

Tests of polarization error made at the antenna laboratory 830 feet from the VOR, agreed with other ground tests made with a polariscope<sup>4</sup> at a point 770 feet north of the VOR site. Polarization measurements made in flight confirmed the ground tests. Flight tests were also made to determine bearing error, distance range, and cone width. Flight tests were also made to determine bearing error, distance range, and cone width.

### DESCRIPTION

The Type FTL-21A VOR antenna is a vertical cage type array which is relatively easy to set up and adjust. A view of the antenna installed on top of a counterpoise is shown in Fig. 1. The structure consists of an upper cage A, and a lower cage B. The latter is enclosed in a removable fiber glass cover. The lower cage contains inner and outer radiating cavities, which together form a concentric radial wave guide system. Figures 2, 3, 4, and 13 are views of the lower cage B. Two vertical dummy X-band wave guides C, extending the entire length of the upper and lower portions of the array and 18 aluminum tubes D, which comprise the outer portion of the lower cage, are set in a circle 25 1/2 inches in diameter. The rectangular wave guides are disposed diametrically opposite each other. The inner portion of the lower cage consists of 20 vertical aluminum tubes arranged in a circle 16 inches in diameter. The outer and inner portions of the lower cage are secured by clamping members to a mounting flange E, and to an upper flange F. The over-all height of the lower cage is 6 feet.

The carrier antenna disc G, along with its matching stubs or "cluster" H, a stiffening disc I, (made of insulating material) and a circular inductive tuning iris J, are all included in the lower cage assembly as it is shipped from the factory. The rotating dipole assembly K, is placed in position from the bottom after the cage is installed.

The outer portion of the upper cage L, consists of 18 aluminum tubes and two rectangular dummy wave guides so arranged that they appear to be extensions of the corresponding elements of the outer portions of the lower cage. The over-all length of these elements is 12 feet and they are secured to upper and lower mounting discs M and N, by clamping members. An inner concentric assembly 16 inches in diameter made of 10 vertical aluminum tubes 8 feet long is also included. The inner assembly is secured to the lower mounting disc N, an intermediate disc O, and a second disc P, by means of the same type clamping members used in other portions of the upper and lower cages. Discs O and P, in addition to stiffening the entire upper cage, also serve to detune the radial wave guide system formed by the vertical rods and the mounting discs M and N. Nylon guy ropes for the structure are attached to the intermediate disc P. An inidite finish has been applied to all of the aluminum rods used in both the upper and lower cages.

<sup>4</sup> Sterling R. Anderson and Wendell A. Iaw, "The Measurement of VOR Polarization Errors," CAA TD Report No. 202, May, 1953

The rotating dipole assembly is shown in Figs. 4, 5, and 6. Figure 5 shows it in an inverted position with the fiber glass cover Q, still in place. Sideband energy is supplied to the dipole through fitting R, and 110-volt 60-cps power for the 1/16 hp, 1800-rpm synchronous motor fed through fitting S. A 9960-cps tone wheel wheel is mounted on the same shaft as the dipole. Energy from the tone wheel is available at terminal T. The rotating  $1/10$  wavelength dipole U, is shown in Fig. 6. Sideband energy, fed at point R, Fig. 5, is supplied to the rotating dipole through a capacity-coupled rotating joint of low characteristic impedance. A series inductive stub cancels out the capacity of the rotating joint.

Inasmuch as it was desired to rotate the entire array during part of the evaluation tests, the assembly was mounted on a rotatable mechanism, the top plate V, of which may be seen in Figs. 2 and 4. Figure 7 shows the rotating pedestal from inside the transmitter building. To rotate the antenna array, it was necessary to raise the antenna and the mounting plate by means of the bar lever W, and to produce the desired angular movement by turning the handle X, of the geared rotating mechanism. Clamps were provided inside the building to assure good bonding between the array-mounting plate and the counterpoise. In practice these were not used, as gravity provided adequate pressure for good bonding. The matching stubs used on the carrier line are enclosed in the cover Y, which may be seen in Fig. 7.

The carrier antenna disc G, in the lower cage is supplied with rf energy through one of the 20 hollow aluminum tubes forming the inner portion of the lower cage. The carrier antenna radiates a circular pattern. The rf phase of the carrier pattern does not change with azimuth. The 9960-cps energy from the tone wheel, frequency-modulated at 30-cps with a deviation of  $\pm 480$  cps, is used to amplitude-modulate the rf energy supplied to the carrier antenna and to provide an FM subcarrier for the reference phase signal. The spinning dipole, whose rf pattern is a figure-of-eight, provides the variable phase voltage for the aircraft receiver. In space the figure-of-eight pattern radiated by the spinning dipole, combines with the circular pattern radiated by the carrier antenna, to produce a rotating pattern shaped like a limaçon. The rf energy supplied to the dipole antenna is taken from the carrier output of the transmitter and then stripped of its modulation by means of a modulation eliminator. This method of obtaining rf energy for the rotating antenna is used in order to reduce the possibility of random variation in phase relationship between rf patterns of the dipole and the disc antenna.

The inductive tuning iris J, is a cylinder 12 inches high which serves as an inductive tuning susceptance with respect to the rotating dipole, and may be considered as a fixed element. The lower cage assembly provides radial resonant chambers for the rf energy from the rotating dipole; and, while re-radiating this energy, reduces its vertical component materially. A further reduction in the vertically polarized energy radiated by the lower cage assembly is effected by the upper cage.

## TESTS AND RESULTS

The tests reported here were conducted on one frequency namely 112.3 Mc. Ground tests of bearing error were made using different methods of measurement. In Fig. 8, curve A shows the bearing errors observed at the counterpoise edge, using a standard CAA VOR monitor. Curve B on Fig. 8 was obtained at the same time as curve A, but using a newly developed TVOR monitor. Curve C was obtained in flight at a 6-mile radius. The data for curves A, B, and C in Fig. 9 were obtained simultaneously. Curves A and B were obtained at the counterpoise edge in conjunction with a standard monitor and a recently developed TVOR monitor respectively. Curve C was obtained at the receiver laboratory while rotating the antenna and using a Collins 51R-2 receiver.

Proper phase relation between the sidebands and carrier was checked by temporarily inserting a 90° length of RG-8/U transmission line in series with the sideband feed line and then adjusting the length of the rf phaser so that a minimum variable phase reading was obtained at the VOR monitor. The added 90° length of line was then removed and the station was assumed to be properly phased. Occasionally, phasing was rechecked after the 90° line was removed by adjusting the phaser for maximum indication on the monitor. Although extremely close agreement in phaser position was obtained by the two methods, the former was preferred because the indication was considerably sharper.

The optimum position of the phaser, as determined with the monitor pick-up unit located on the edge of the counterpoise, was compared with that determined by use of the pick-up unit located 175 feet from the antenna along the same radial. A discrepancy of as much as 20° was noted between the two readings. It was subsequently determined that neither of these positions resulted in the minimum gross error spread. The method finally used for determining proper phaser setting was to obtain a bearing error curve for each of several positions of the phaser, and use that setting which gave the least total bearing error spread. A typical family of curves obtained in this manner is given in Fig. 10. It is believed that cross-coupling between the carrier and sideband antennas is responsible for the above variation. It should be noted that the low bearing error spread of 1.3° obtained in curve C could not be reproduced. Adjusting the shorts in the four slots of the disc antenna by small amounts did not effect any noticeable improvement. It was later found that slightly closer agreement in phaser position, as determined at the two distances from the station, was obtained when the sideband line was carefully matched at point R, Fig. 5.

Curve A of Fig. 11 shows the variation in indicated optimum phaser position with change in azimuth. These data were obtained by moving the pick-up unit around the counterpoise in 20° steps, and rephasing for each position of the pick-up. In order to make the readings as accurate as

possible, a 90° length of line was first inserted in the sideband antenna feed, and the phaser was adjusted for minimum indication on the monitor. A total variation of nearly 7° in phaser position was indicated by this test. Curve B of Fig. 11 shows the phaser position when the 30-cps filters in the monitor were switched out of the circuit.

Some variation in space modulation percentage with azimuth was noted at the counterpoise edge. As will be observed in Fig. 12, the space modulation varied between the limits of 28.7 and 31 per cent. As in the case of the tests made for variation in phaser position with change in azimuth, these readings were obtained by moving the rf pick-up to fixed points 20° apart on the periphery of the counterpoise and reading the modulation percentage on the station monitor.

#### POLARIZATION TESTS

A polarization error of  $\pm 1.91^\circ$  was measured when the antenna system was first set up. This value was a little higher than expected and in addition proved to be somewhat variable. A poorly clamped rod in the lower cage assembly was discovered; so the entire antenna was taken down and all clamping members were tightened as well as possible with the aid of wrenches. Before the upper cage was restored, but with all other adjustments properly made, the measured polarization error was  $\pm 10.35^\circ$ . When the top cage was again installed, the error was reduced to  $\pm 1.9^\circ$  and appeared to be stable. Adding a screen of hardware cloth to the middle section of the upper cage, lowered the polarization error to  $\pm 1.1^\circ$ . This was reduced to  $\pm 0.35^\circ$  by placing hardware cloth screens around the top and bottom sections of the upper cage.

Later, before installing an upper cage, which was modified as shown in Fig. 13 and supplied by the manufacturer, the hardware cloth was removed and the polarization error was measured at  $\pm 1.75^\circ$ . When the new cage, with its three additional shorting discs was installed, the polarization error was reduced to  $\pm 0.92^\circ$ .

#### MISCELLANEOUS TESTS

A comparison of the bearing errors observed with the tone wheel attached to the same drive shaft as the spinning antenna; and, the errors observed when the tone wheel of a standard CAA type goniometer was used to supply the 9960-cps FM energy for the subcarrier, is given in Fig. 14. Although the position of the phaser was not changed during these tests, it was not set at the compromise position which gave minimum error spread, but instead was set at the point which indicated correct phasing between the sideband and carrier when the pick-up unit was located 175 feet from the antenna.

Figure 15 shows a comparison of the error curves obtained when checking the variable phase only. Curve A was obtained when the plate supply of the carrier modulator unit was turned off, thus removing the 9.96 kc FM signal from the rf energy radiated by the antenna system. Curve B shows the errors obtained when the system was operating normally. During this test, the data for both curves at any one azimuth were obtained without moving the pick-up unit.

Figure 16 is the last station error curve obtained at the counterpoise edge after the system had been operating undisturbed for ten days. During this period, the station error curve varied between  $2.1^{\circ}$  and  $2.6^{\circ}$  spread. The standard CAA monitor with 30-cps filters was used while making this series of tests.

### FLIGHT TESTS

The flight tests conducted on the FTL-21A VOR antenna consisted of polarization checks, distance range checks, theodolite orbits and cone measurements. For comparison purposes the flight test data obtained on the CAA four-loop VOR antenna with polarizer are listed with the FTL-21A antenna data.

#### Polarization Flight Checks

In flight testing the VOR antenna three polarization tests were conducted. These tests were made at a distance of approximately 20 miles from the VOR station at an altitude of 1,000 feet above ground in a Douglas C-47 aircraft using a Collins 51R-2 receiver and a tail-mounted V-109 receiving antenna. A description and results of the tests performed follow:

#### 1. 30-degree wing rock

Headed toward the station, the aircraft was banked  $\pm 30^{\circ}$ . The nose of the airplane was held "on the point" during this maneuver. The course deviation indicator current was recorded and converted to degrees of course displacement.

|               |                   |
|---------------|-------------------|
| FTL-21A       | $\pm 0.4^{\circ}$ |
| CAA four-loop | $\pm 0.5^{\circ}$ |

#### 2. Eight ways over ground check point

Recording the course deviation indicator current, the aircraft was flown on eight different headings (crossing a point at every  $45^{\circ}$  heading) over a specific ground check point. The recording was marked

as the airplane crossed the check point and the indicated bearing was compared with the magnetic bearing. The zero reference point in each case was taken on the heading to the station.

|               |                 |
|---------------|-----------------|
| FTL-21A       | $\pm 0.6^\circ$ |
| CAA Four-Loop | $\pm 0.6^\circ$ |

### 3. Circle Test

The method employed in measuring the error in the circle test was as follows:

Headed toward the VOR and starting from a ground check point, a circle was flown at a constant  $30^\circ$  bank. The course deviation indicator current was recorded during this circle and converted into degrees of error from the azimuth course which was being flown at the beginning of the circle. Since the aircraft in the circular flight was changing azimuth with respect to the VOR, this deviation was computed in degrees and subtracted from the course deviation indicated error, resulting in the numerical value of polarization error, following the removal of the receiver error.

|               |                 |
|---------------|-----------------|
| FTL-21A       | $\pm 0.9^\circ$ |
| CAA Four-Loop | $\pm 0.5^\circ$ |

### Distance Range Flight Check

The distance range of a VOR facility is defined as the distance in statute miles from a VOR at which the course width in degrees becomes double the course width measured at ten miles from the VOR. This test is conducted at an altitude of 1,000 feet above ground. The distance range flight checks were conducted on the zero radial of the TDEC north omnirange site.

| <u>Antenna</u> | <u>Distance Range</u>           |                                 |
|----------------|---------------------------------|---------------------------------|
|                | <u>Headed North<br/>(Miles)</u> | <u>Headed South<br/>(Miles)</u> |
| FTL-21A        | 60.3                            | 62.0                            |
| CAA Four-Loop  | 61.0                            | 62.3                            |



### Theodolite Flight Calibration

The theodolite flight calibration is a process wherein a series of exact differences between indicated and magnetic bearing are obtained throughout the 360° around a range station. These differences are plotted as a measured error curve. Flights were made in a counterclockwise direction at a 6-mile radius. The measured error curves of the FTL-21A and CAA four-loop antennas are shown in Fig. 17. The numerical error spreads are as follows:

|               |                  |
|---------------|------------------|
| FTL-21A       | $\pm 1.10^\circ$ |
| CAA Four-Loop | $\pm 0.95^\circ$ |

### Cone Measurements

Radial flights were made across the VOR, recording the currents of the course deviation indicator and the TO-FROM indicator of a Collins 51R-2 receiver for the purpose of measuring cone width.

In order to measure the width of the cone from a recording of the course deviation indicator current, a definition of the cone must be stated so that the beginning and end points of the cone may be positioned on the recording. With the VOR receiver and associated recording equipment calibrated to a given recorder deviation equal to a given number of degrees of VOR course displacement, a flight track directly over the VOR is flown. When the course deviation indicator deviates more than 2°, and this deviation (as observed on the recording) is due to the normal course disturbances encountered above a VOR, the cone is considered to begin at this point. In a similar manner the cone ends at the 2° deflection point as the straight line course indication is resumed on the other side of the cone. When measuring a cone in this manner, the results are referred to as a course deviation indicator (CDI) cone measurement.

In this report the TO-FROM cone angle is defined as follows: a flight is made directly over the VOR while recording the TO-FROM indication. The TO-FROM cone angle above ground is the angle between ground and the first point where the TO-FROM indication becomes ambiguous. See Figs. 20 and 21.

Listed below are the average results of the cone measurements on the FTL-21A antenna together with the average of numerous measurements recorded on the CAA four-loop antenna.

## FTL-21A

| <u>Type<br/>Measurement</u> | <u>Cone Angle Above<br/>Ground (Degrees)</u> |
|-----------------------------|--|
| TO-FROM                     | 83.8   |
| CDI                         | 68.2   |
| <u>CAA FOUR-LOOP</u>        |  |
| TO-FROM                     | 90.0   |
| CDI                         | 75.0   |

Figures 18, 19, 20, and 21 are reproductions of recordings, obtained during flight tests, of both course deviation indicator and TO-FROM indicator currents on the FTL-21A and the CAA four-loop antennas. From these recordings, it will be noted that the CAA four-loop TO-FROM indication provides a precise check when the aircraft is directly over the VOR, while the FTL-21A has two periods of time where the TO-FROM indicator provides erroneous information.

## CONCLUSIONS

1. The bearing error of the FTL-21A spinning antenna is nominally within  $\pm 0.85^\circ$  when phased for minimum error.
2. The cone angle above ground is  $68.2^\circ$  as measured by the CDI method and  $83.8^\circ$  as measured by the TO-FROM method.
3. The stability of the system is satisfactory.
4. Polarization error is acceptable when additional discs are installed in the upper cage.
5. The system is relatively easy to install.
6. The nylon guy ropes will require periodic tightening because of stretching.
7. Distortion of the antenna structure due to high winds can produce some course instability.

8. The adjustment of the phaser which gives minimum station error is difficult to determine unless means are provided to make bearing error measurements at the edge of the counterpoise.

9. The clamping members used to secure the vertical tubes to the mounting flanges and discs in both the upper and lower cages do not provide reliable electrical bonding.

10. The distance range of the system is satisfactory.

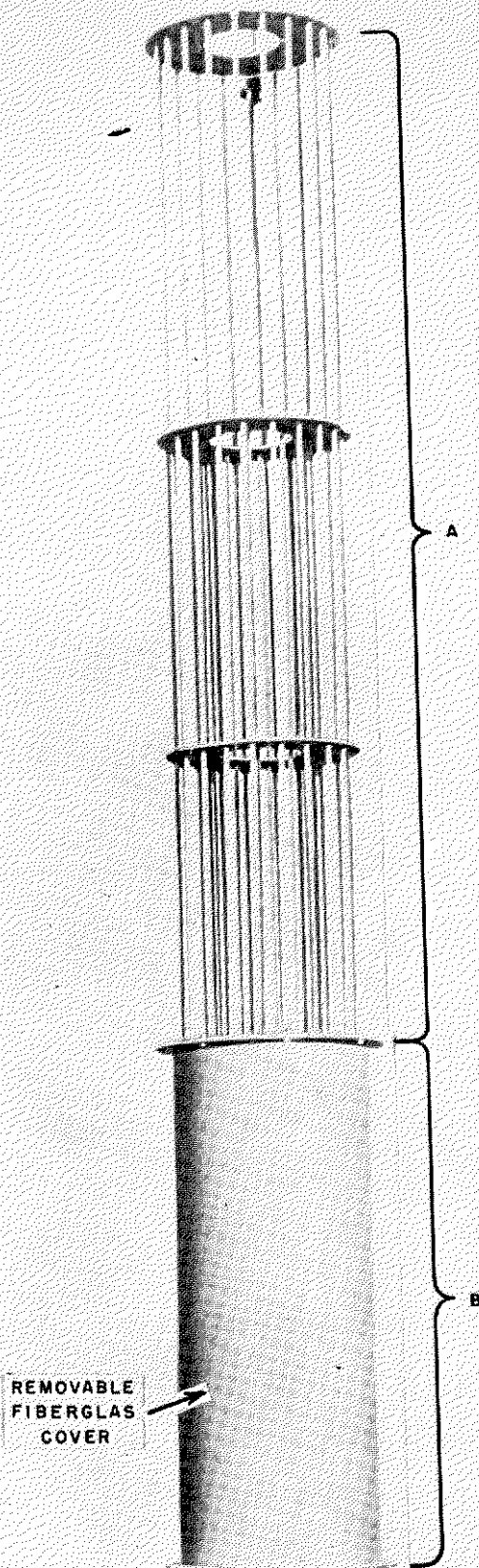


FIG. 1 THE FTL-21A VOR ANTENNA

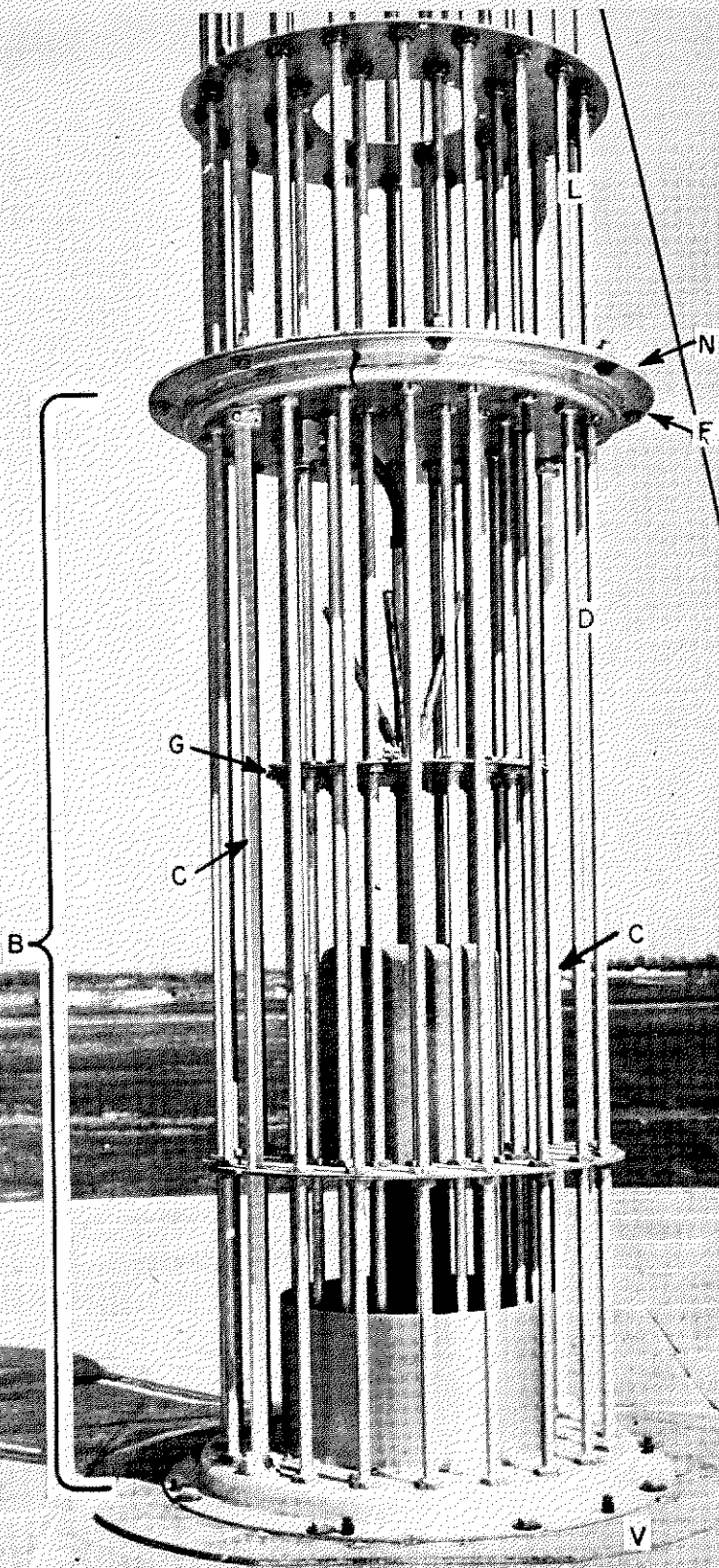


FIG. 2 TOWER CAGE OF FTL-21A VOR ANTENNA  
WITH FIBERGLAS COVER REMOVED



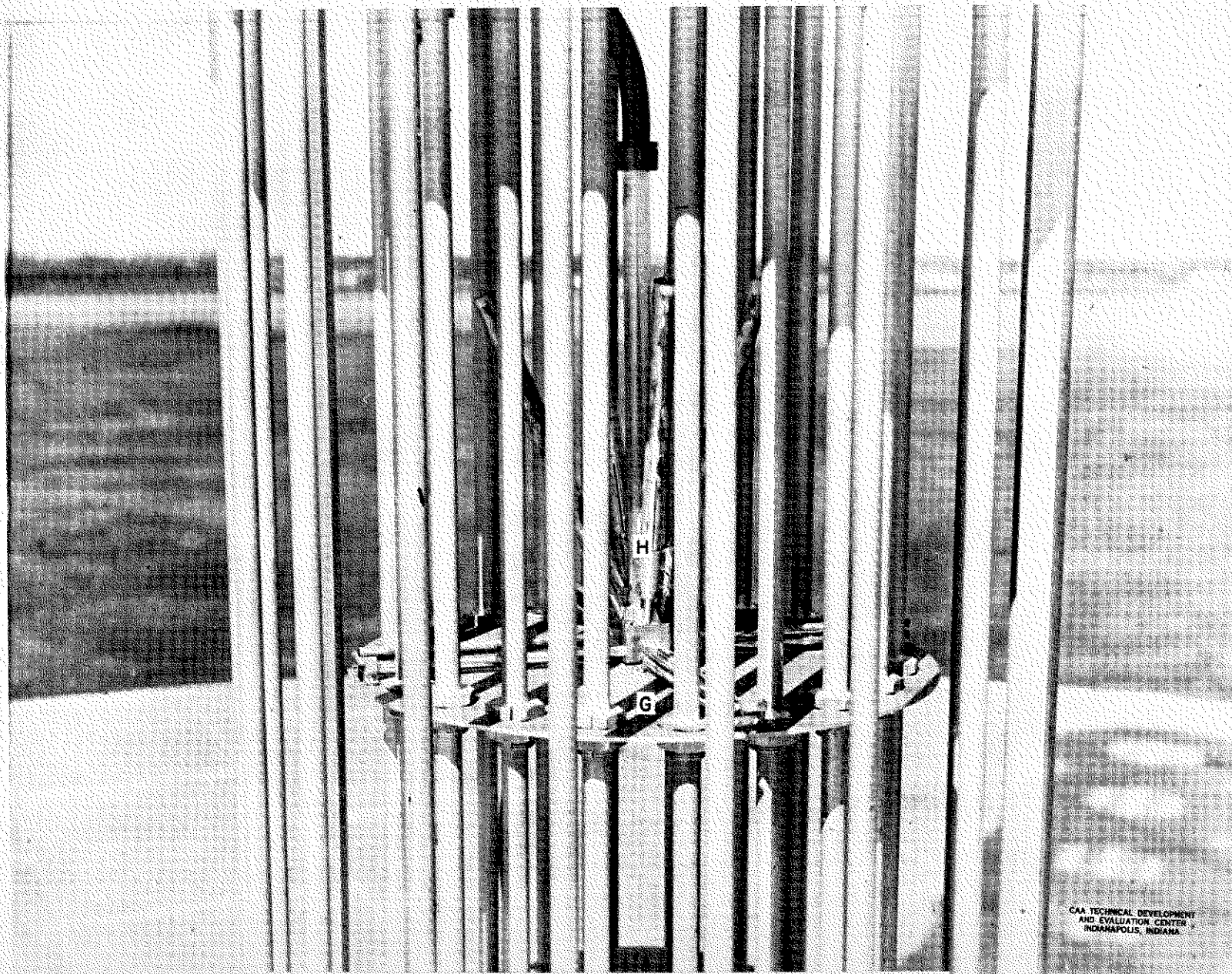
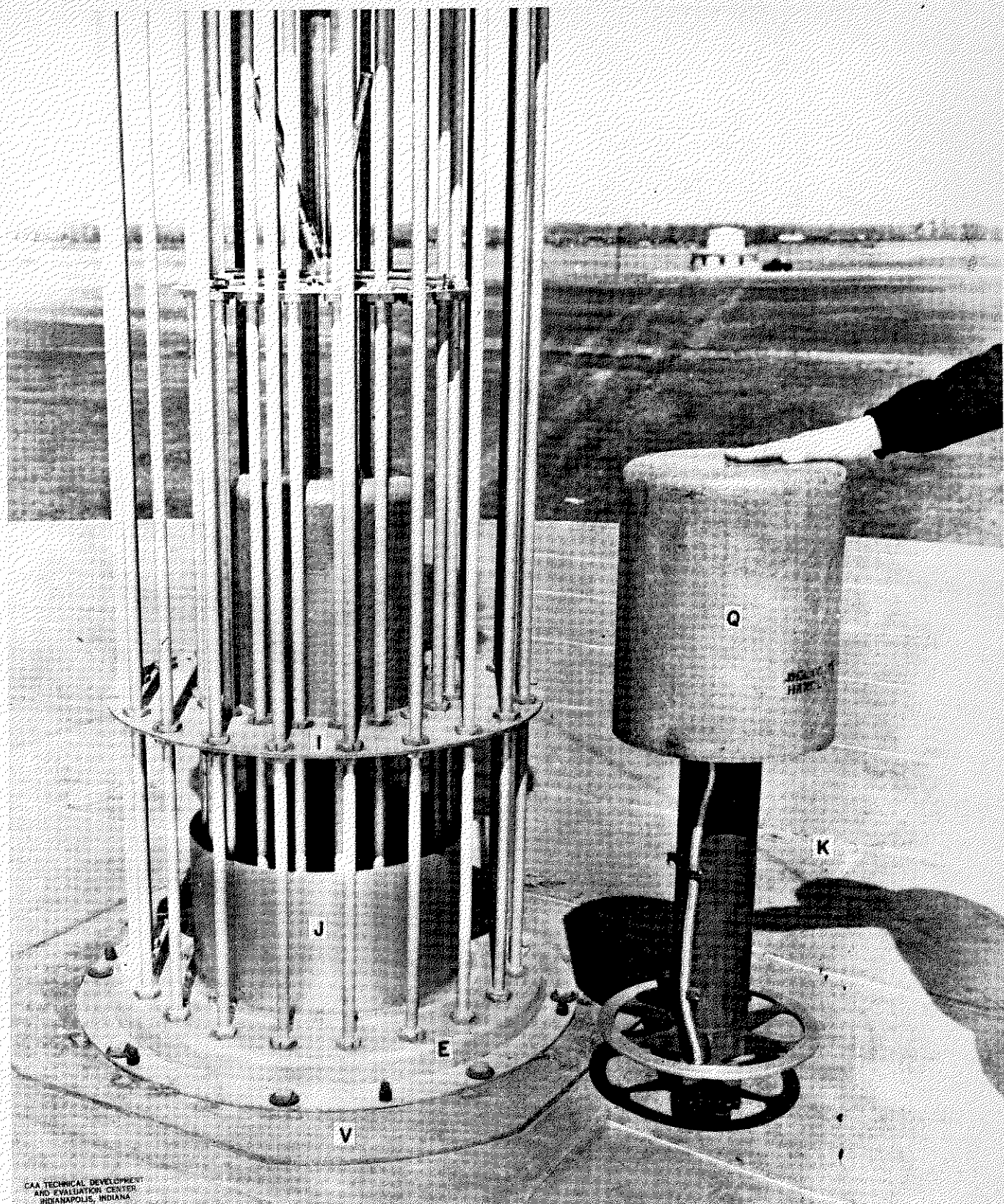


FIG. 3 CLOSE-UP OF REFERENCE ANTENNA AND  
MATCHING STUBS OF FTL-21A VOR ANTENNA



CAA TECHNICAL DEVELOPMENT  
AND EVALUATION CENTER  
INDIANAPOLIS, INDIANA

FIG. 4 SPARE ROTATING DIPOLE ASSEMBLY AND PORTION  
OF LOWER CAGE OF FTL-21A VOR ANTENNA



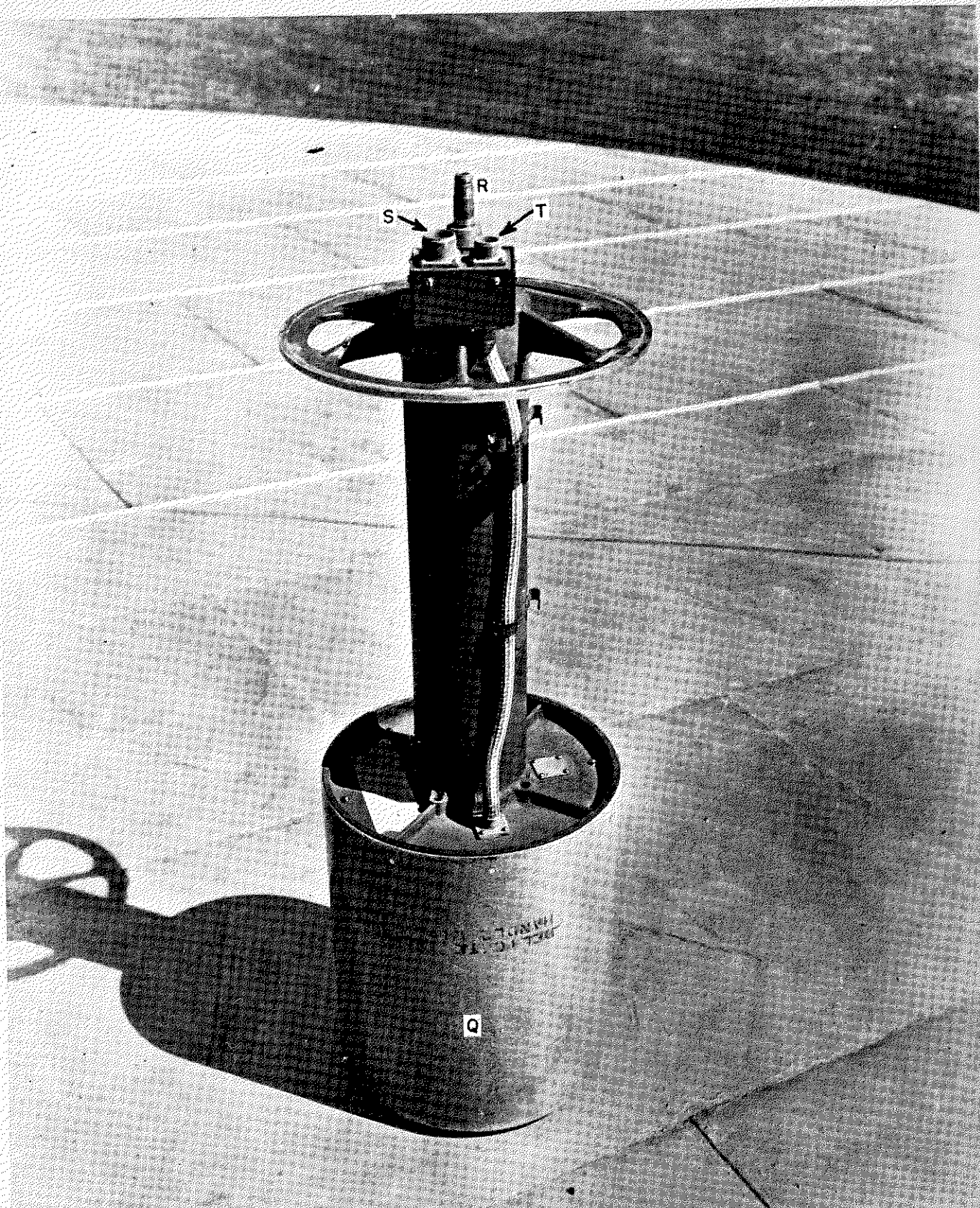


FIG. 5 ROTATING DIPOLE ASSEMBLY REMOVED FROM FTL-21A VOR ANTENNA



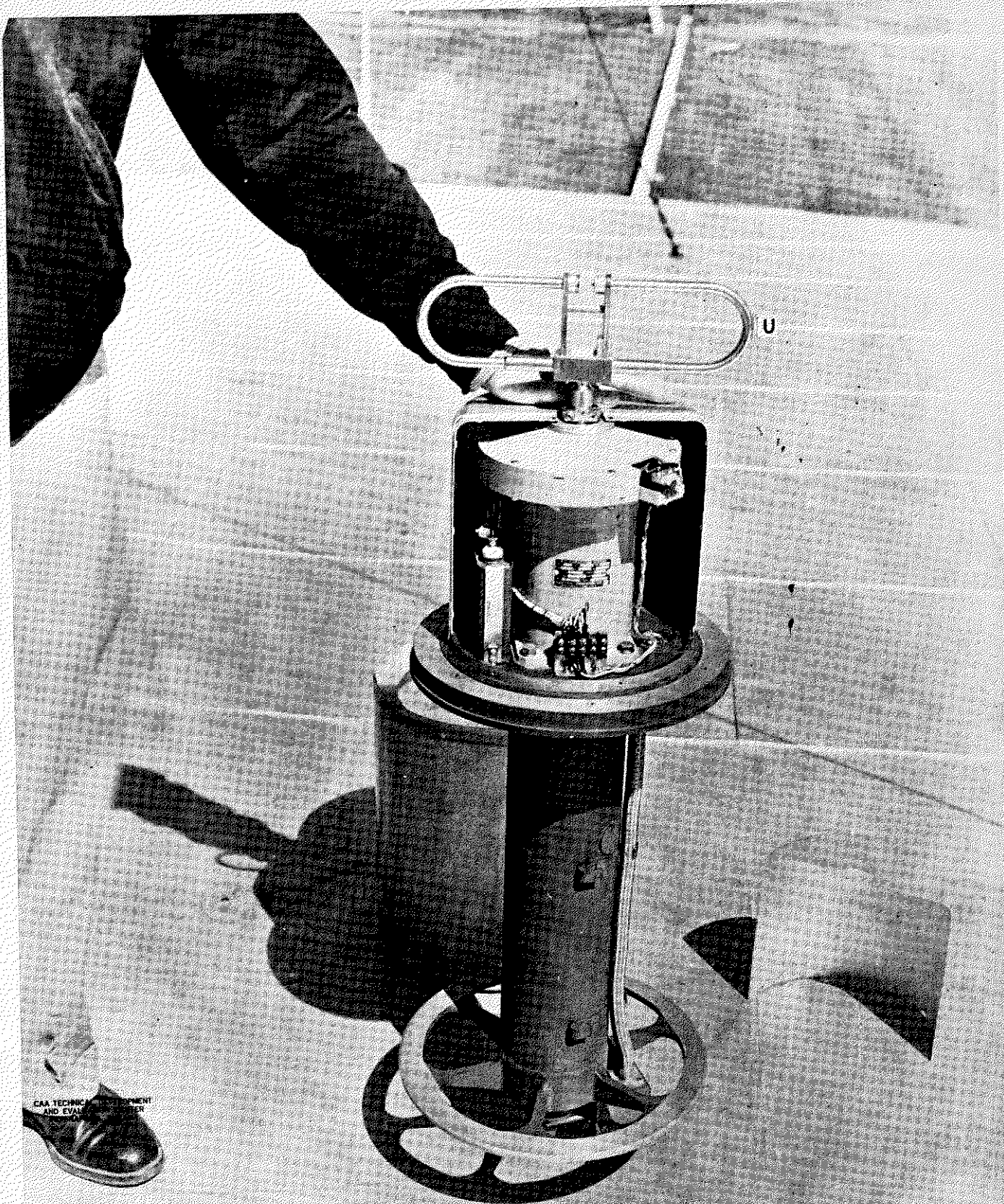


FIG. 6 CLOSE-UP OF FTL-21A VOR ANTENNA ROTATING DIPOLE ASSEMBLY WITH HOUSING PARTIALLY REMOVED

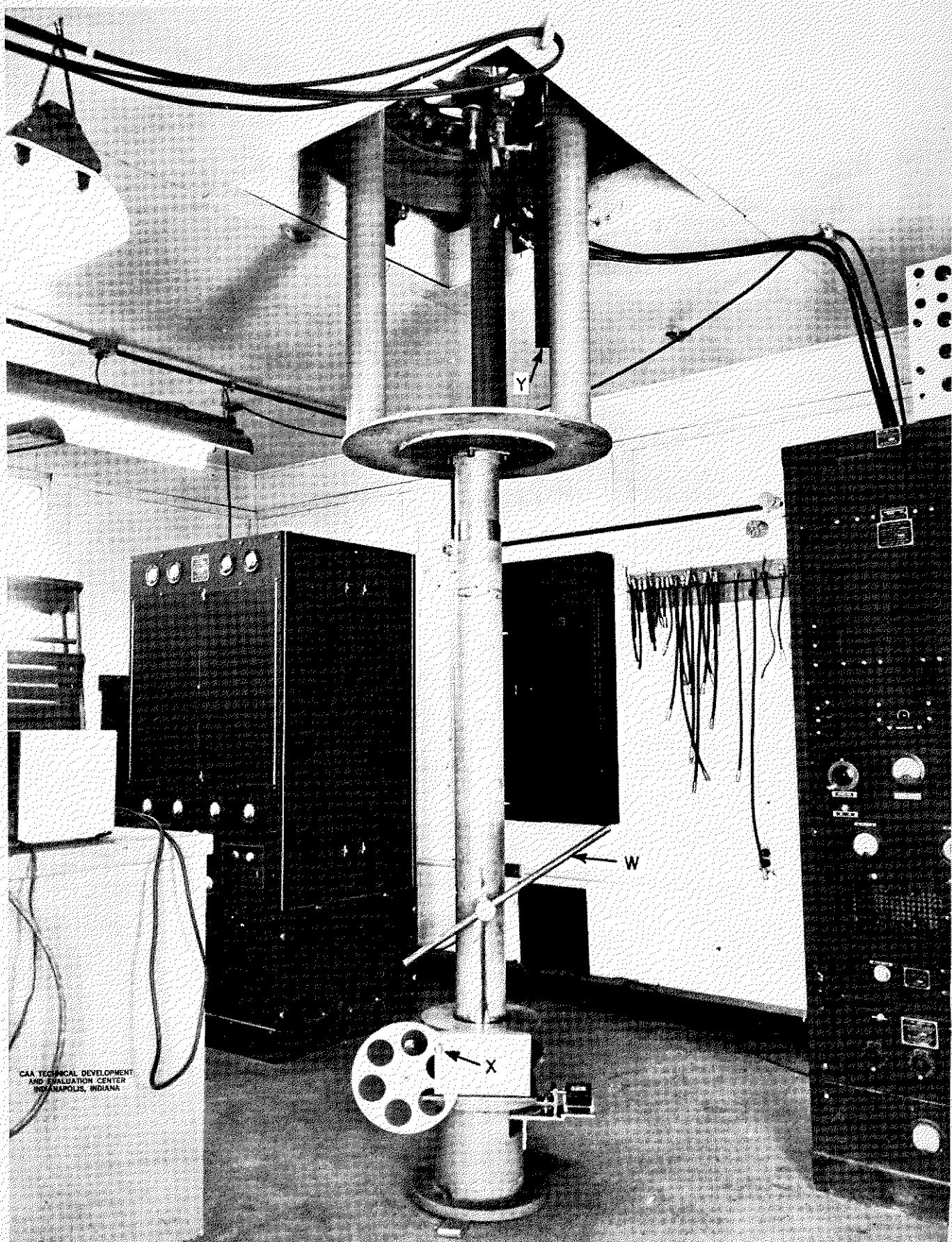
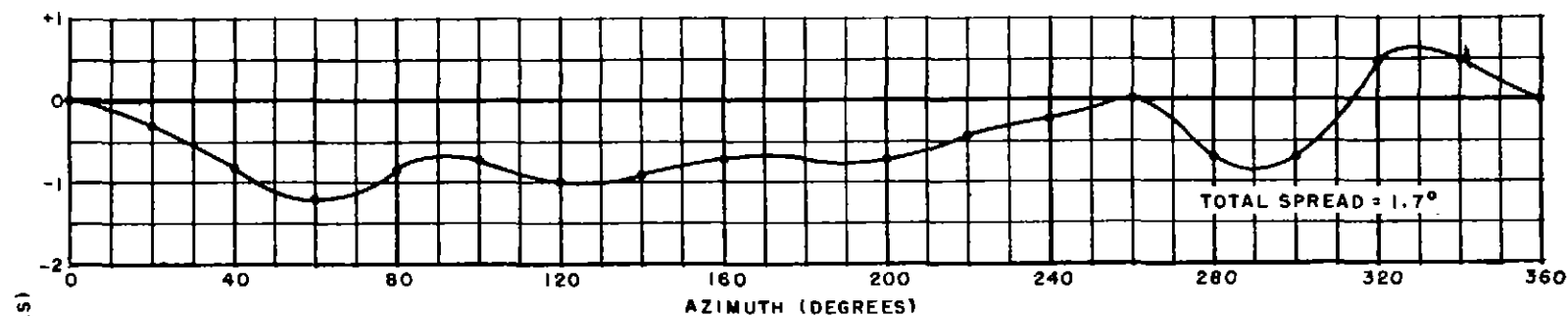
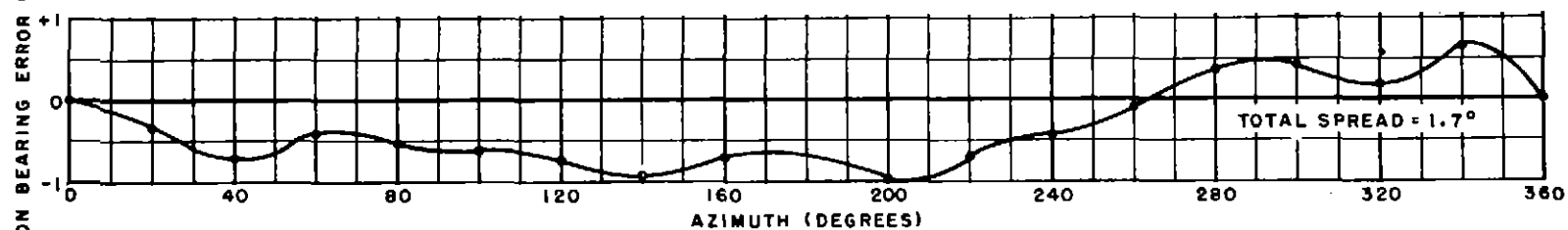


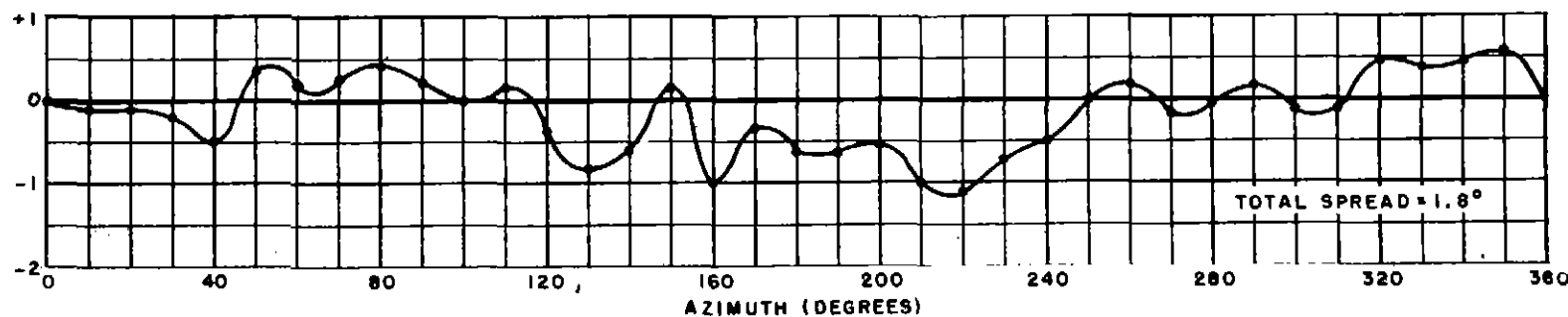
FIG. 7. MECHANISM FOR ROTATING ANTENNA UNDER TEST



(A) STANDARD MONITOR



(B) TVOR MONITOR



(C) AIRPLANE RECEIVER

FIG. 8 STATION BEARING ERROR WITH FTL-21A ANTENNA STATIONARY AND PICKUP MOVED

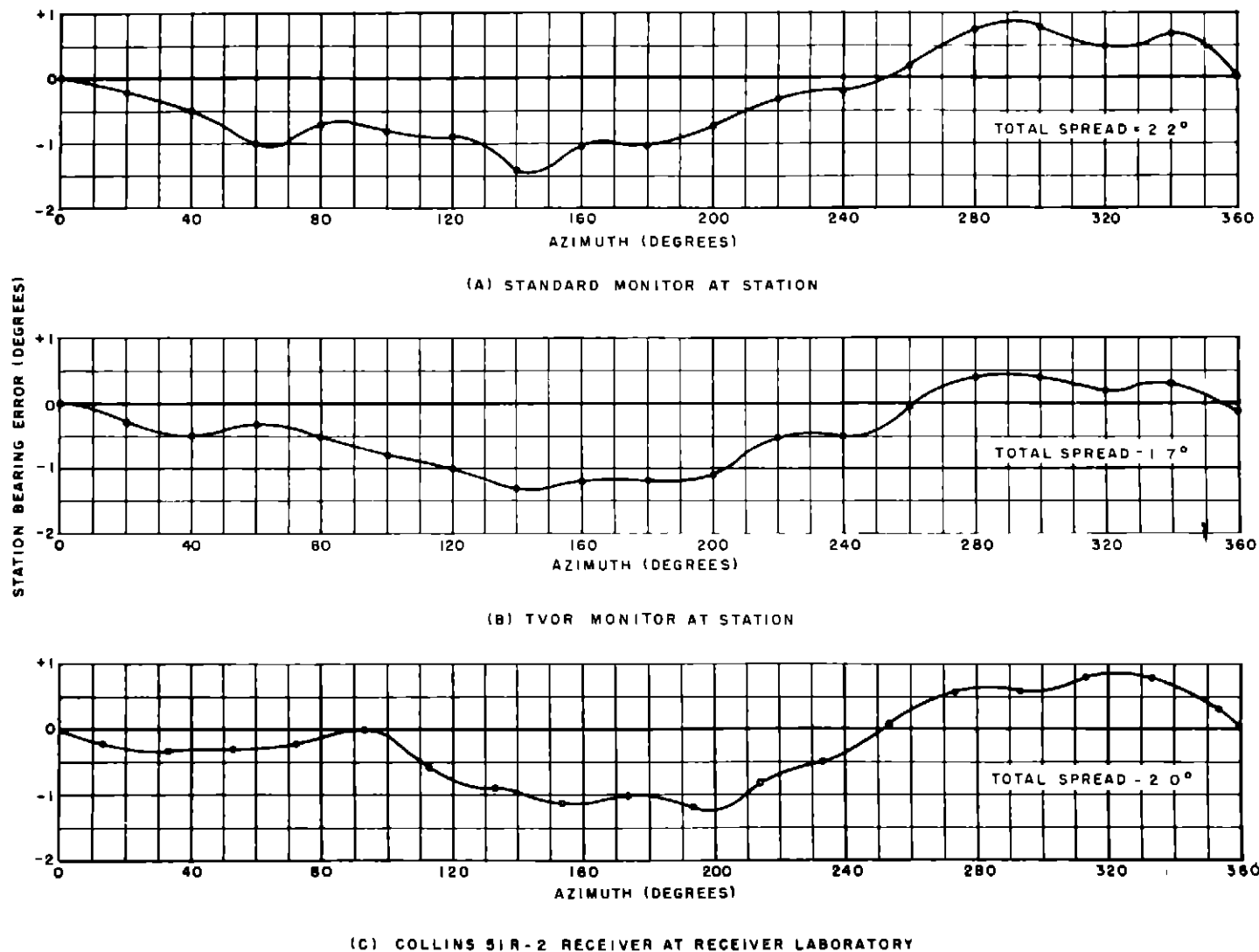


FIG 9 STATION BEARING ERROR WITH MONITORS FIXED AND FTL-21A ANTENNA ROTATED

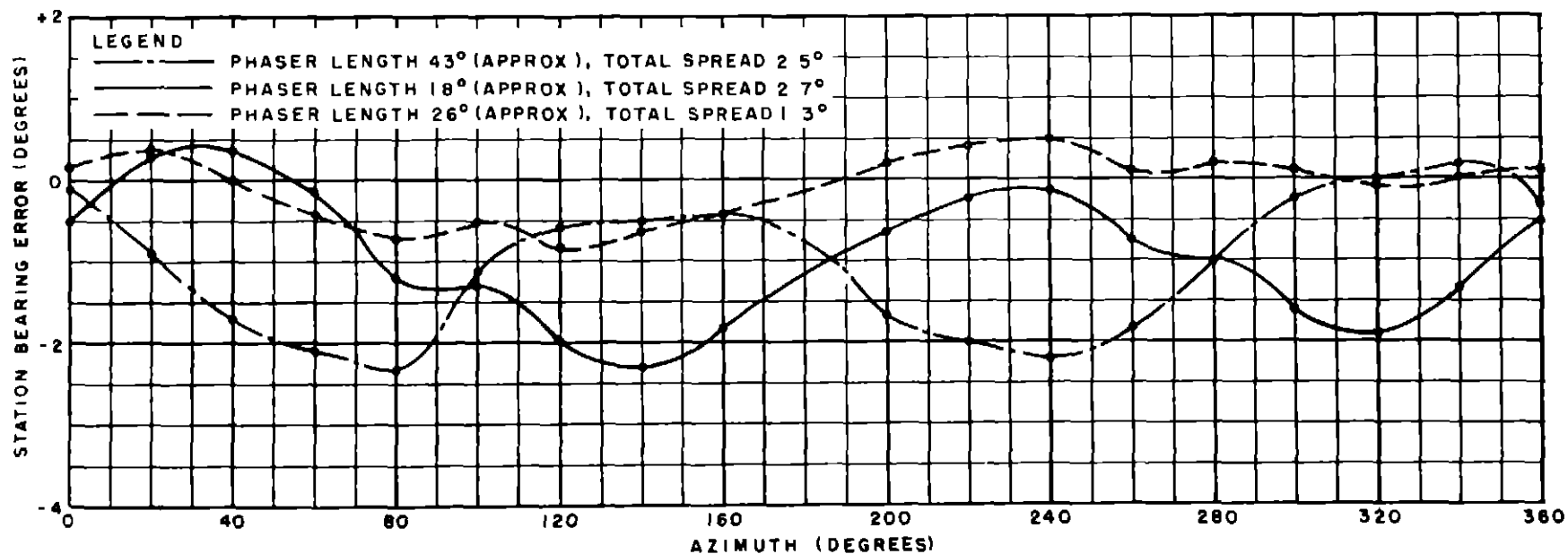


FIG 10 EFFECT OF PHASER POSITION ON STATION BEARING ERROR

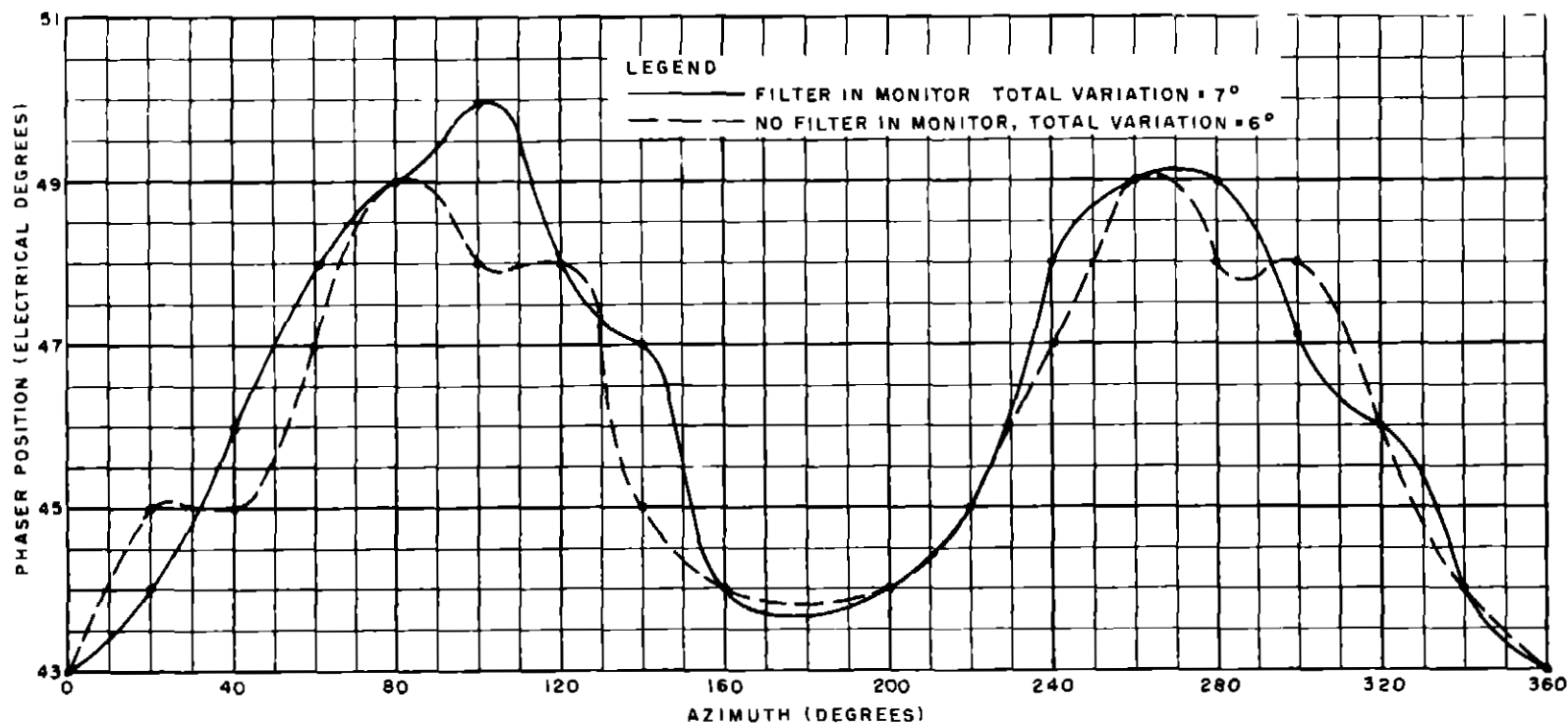


FIG 11 VARIATION OF PHASER POSITION WITH AZIMUTH FOR INDICATED PROPER PHASING

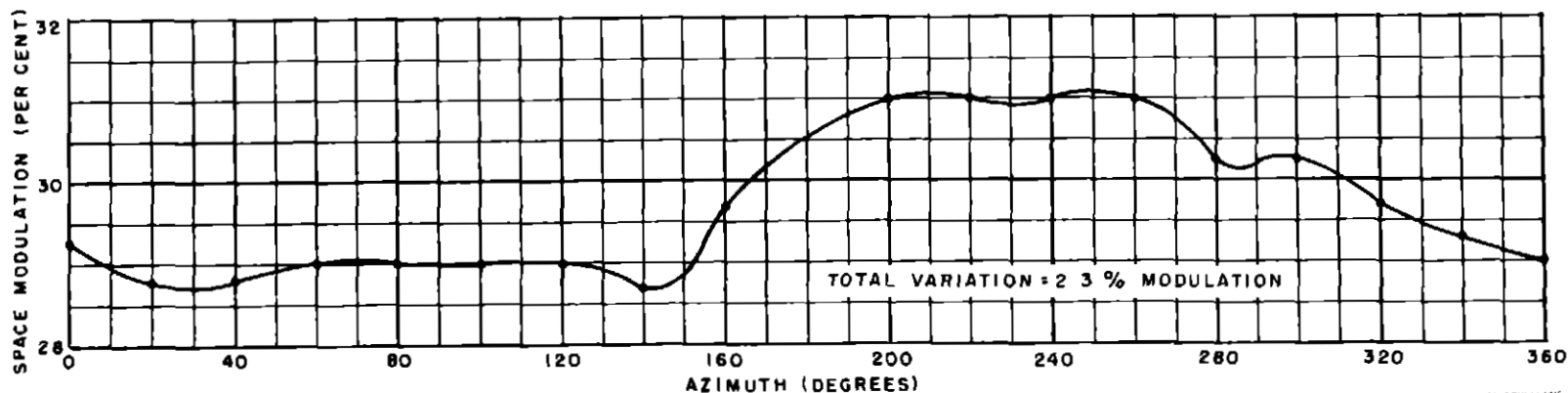


FIG 12 VARIATION OF SPACE MODULATION PERCENTAGE WITH AZIMUTH



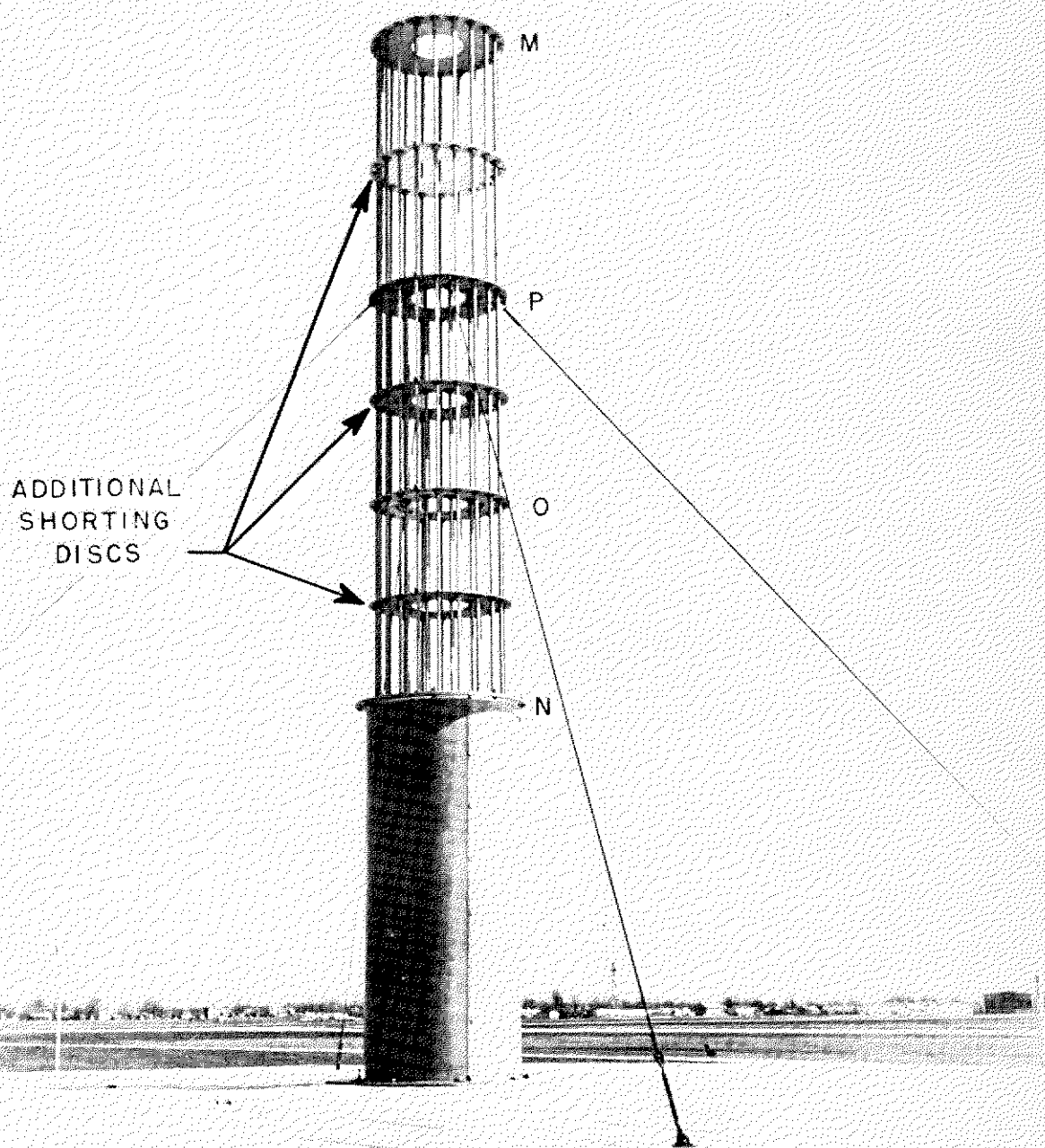


FIG. 13 THE FTL-21A VOR ANTENNA SHOWING  
ADDITIONAL SHORTING DISCS

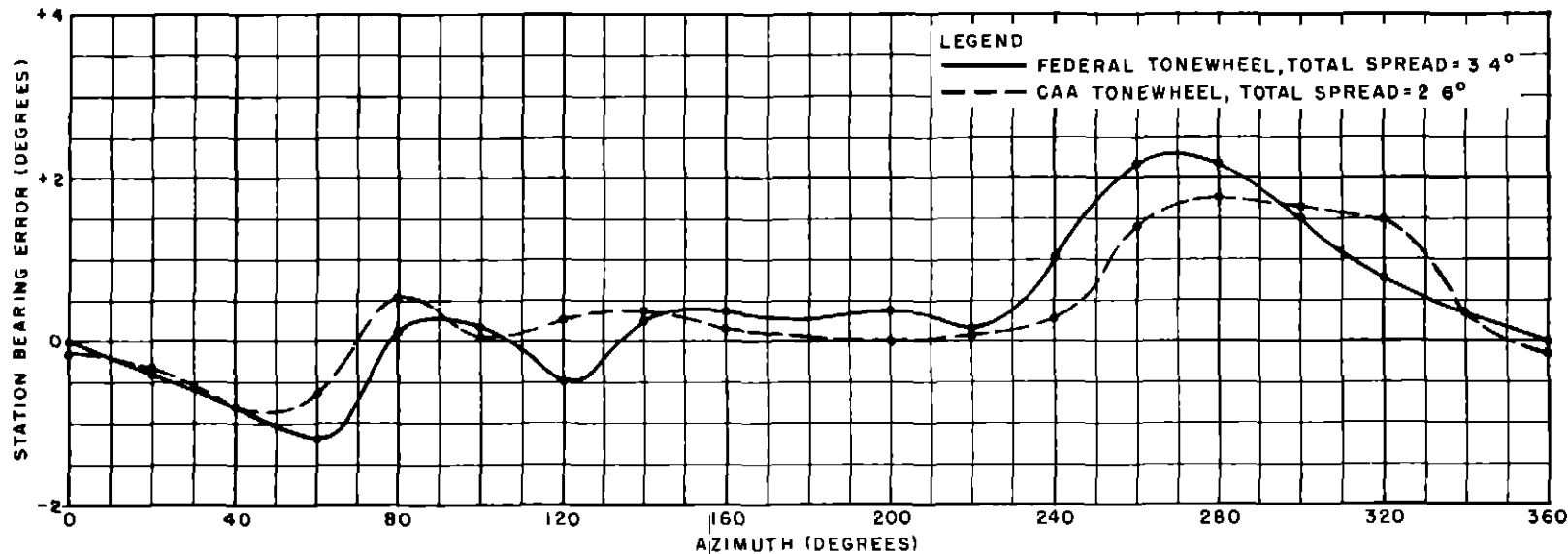


FIG 14 COMPARISON OF BEARING ERROR USING  
FEDERAL AND CAA STANDARD TONERWHEELS

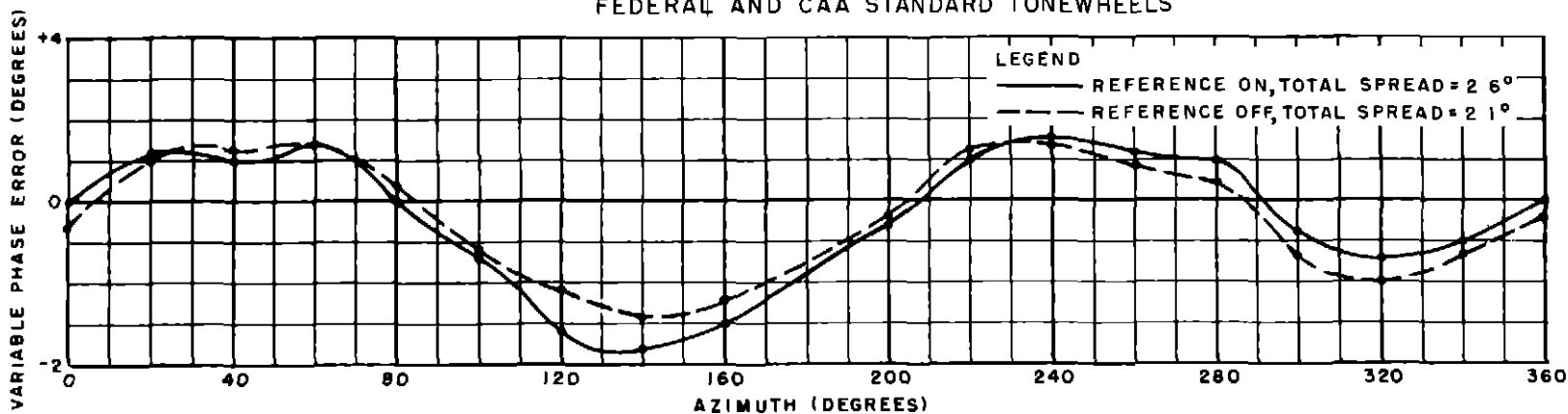


FIG 15 VARIABLE PHASE ERROR ONLY OF FTL-21A VOR ANTENNA



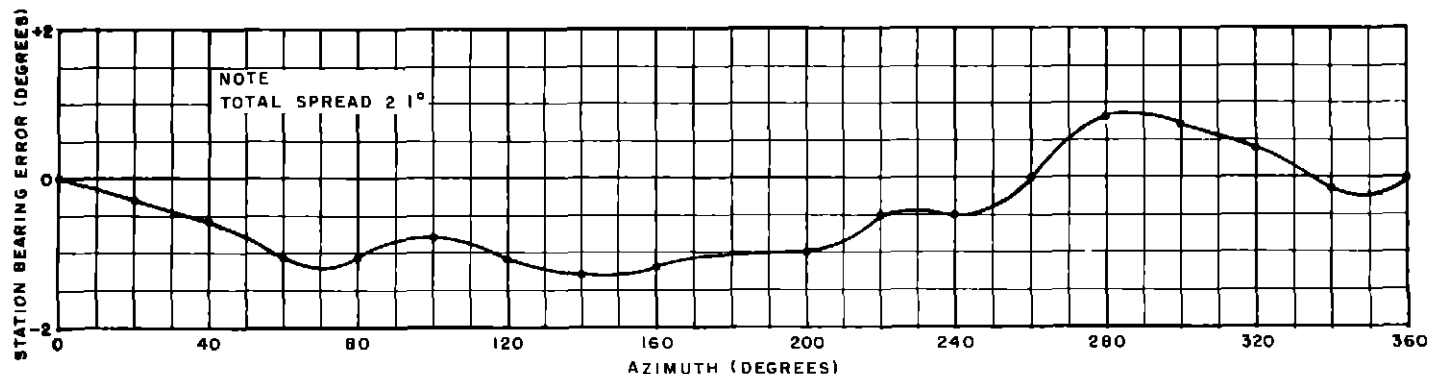


FIG 16 FINAL STATION BEARING ERROR CURVE, FTL-21A VOR ANTENNA

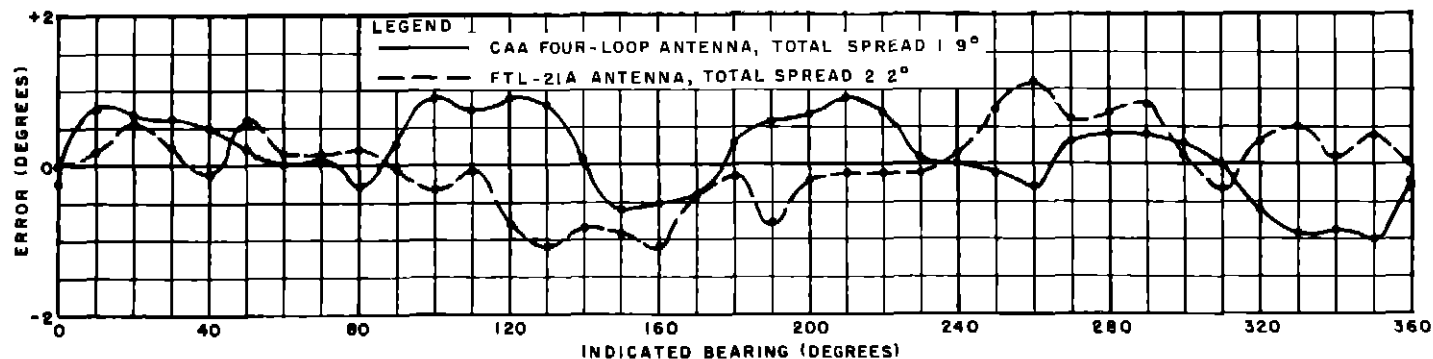


FIG 17 THEODOLITE FLIGHT CALIBRATIONS OF FTL-21A  
AND CAA FOUR-LOOP VOR ANTENNAS

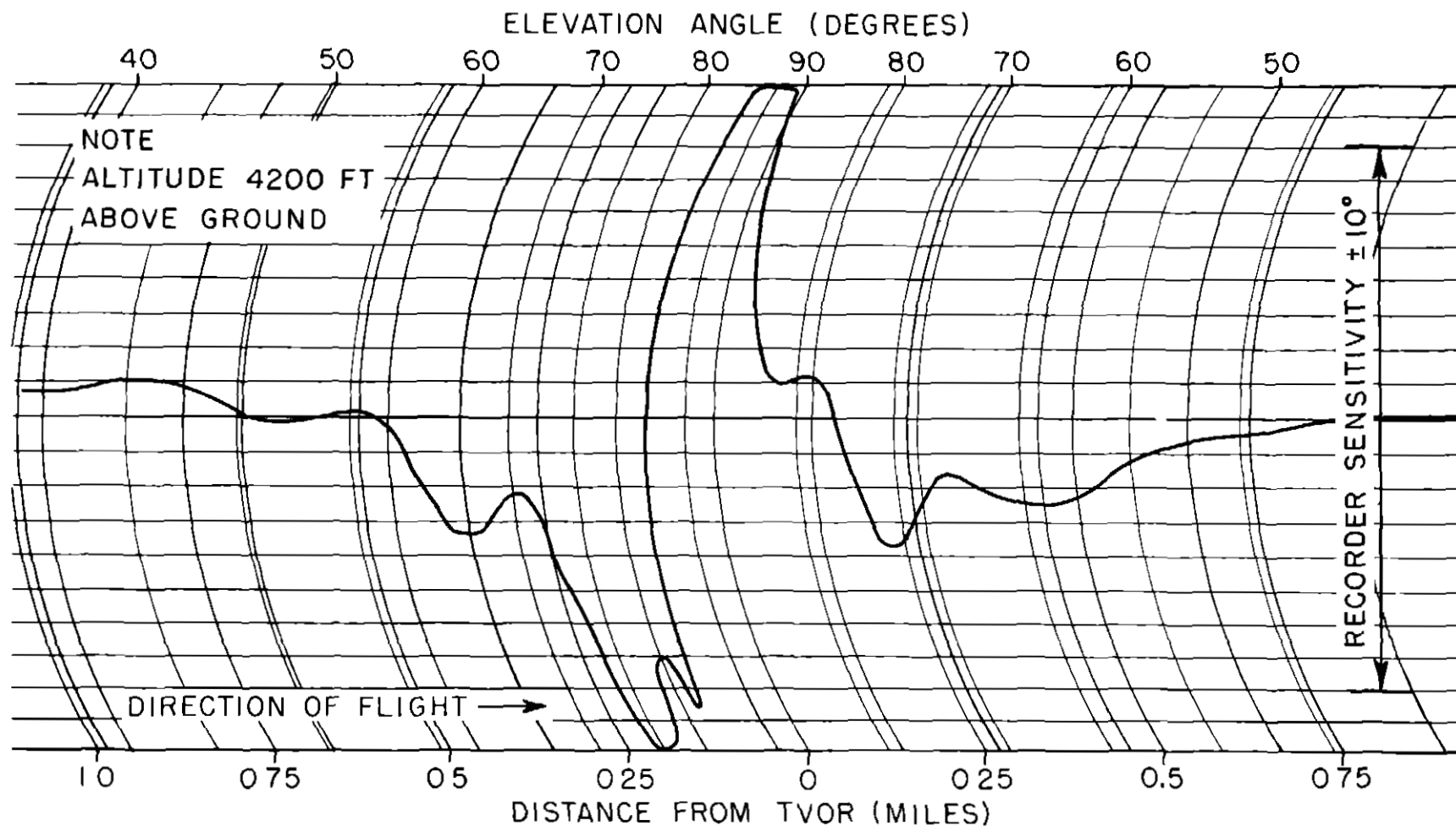


FIG. 18 COURSE DEVIATION INDICATOR RECORDING  
OF FTL-21A VOR ANTENNA

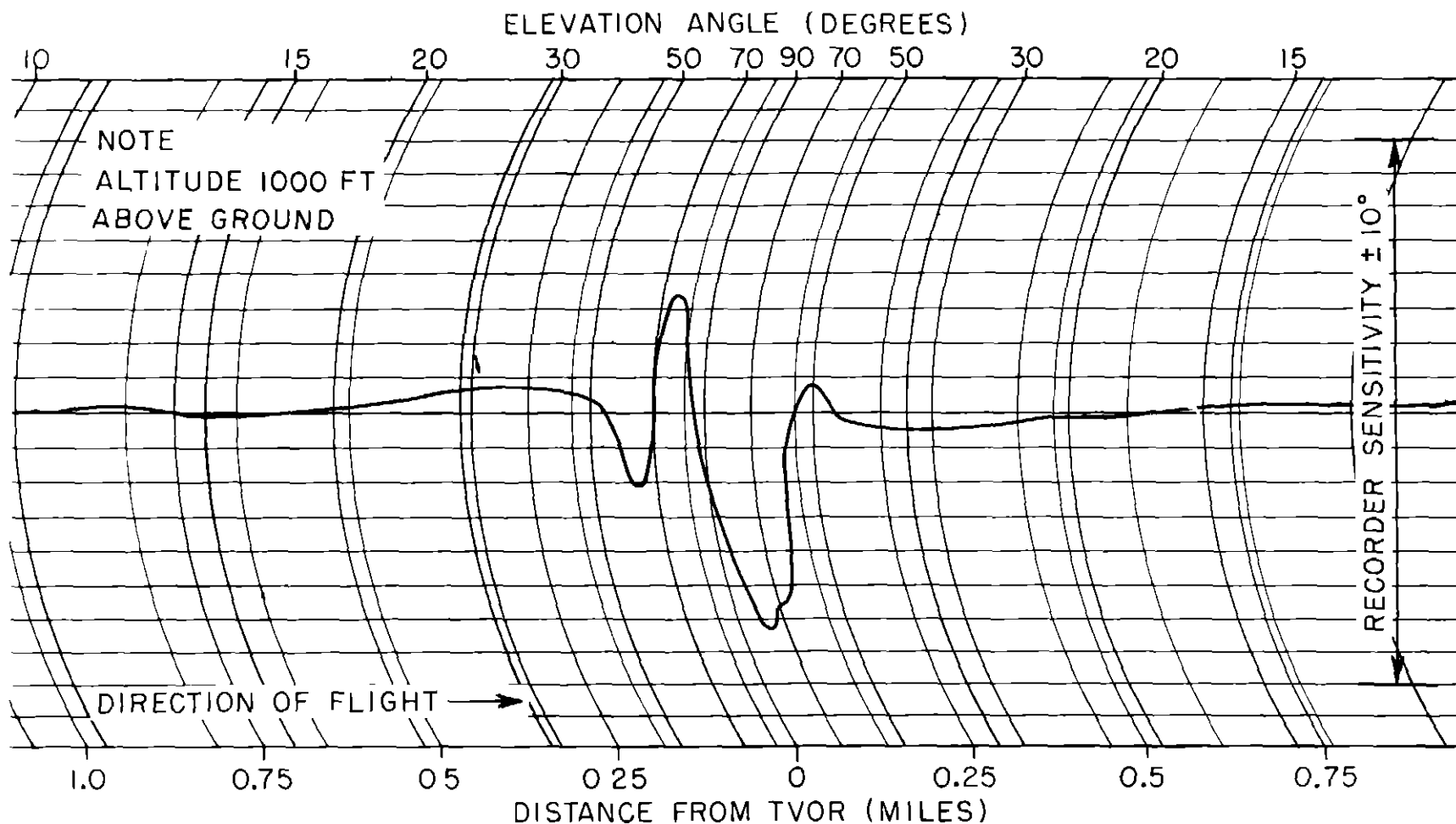


FIG. 19 COURSE DEVIATION INDICATOR RECORDING  
OF CAA FOUR-LOOP VOR ANTENNA

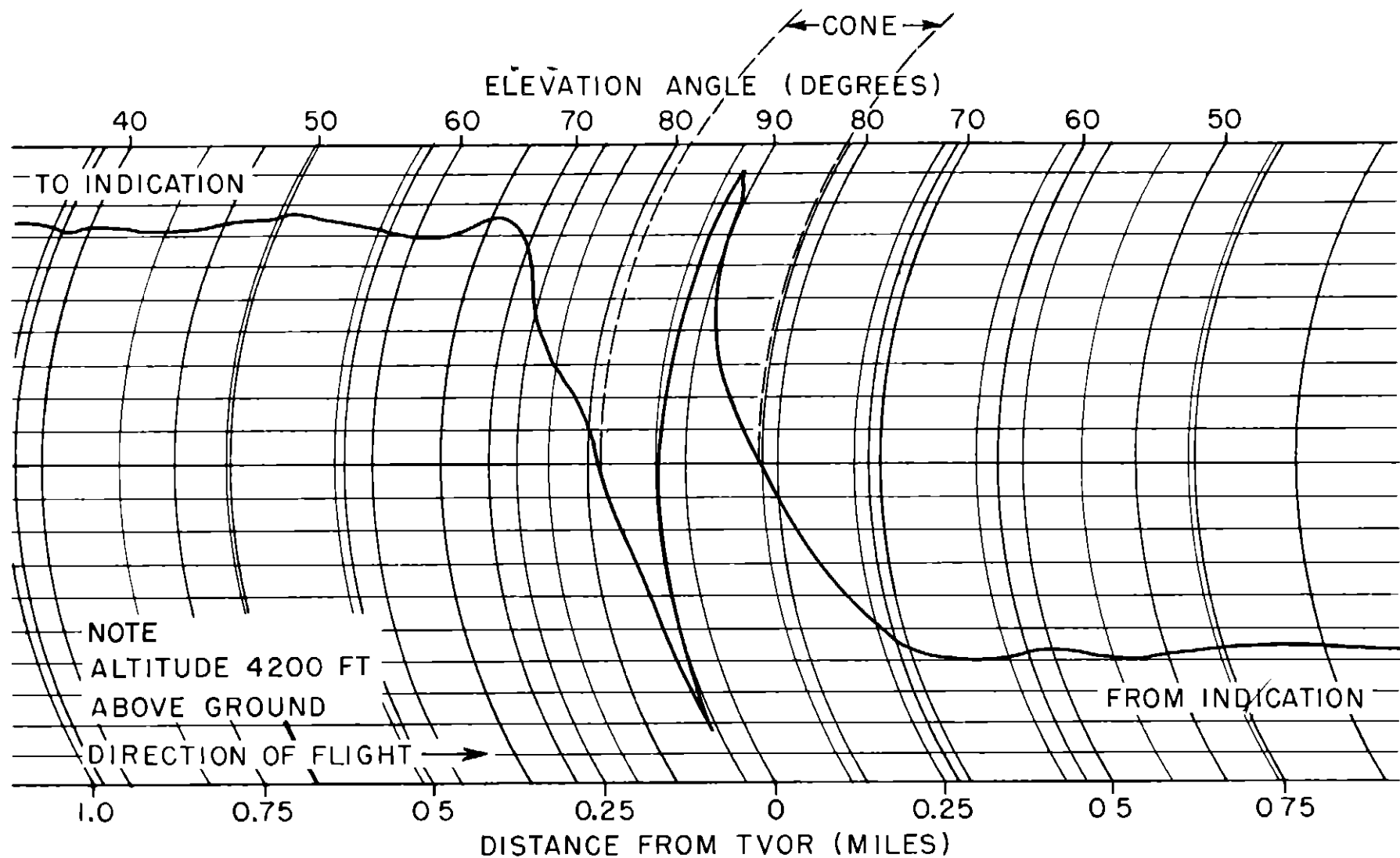


FIG. 20 TO-FROM INDICATOR RECORDING OF  
FTL-21A VOR ANTENNA

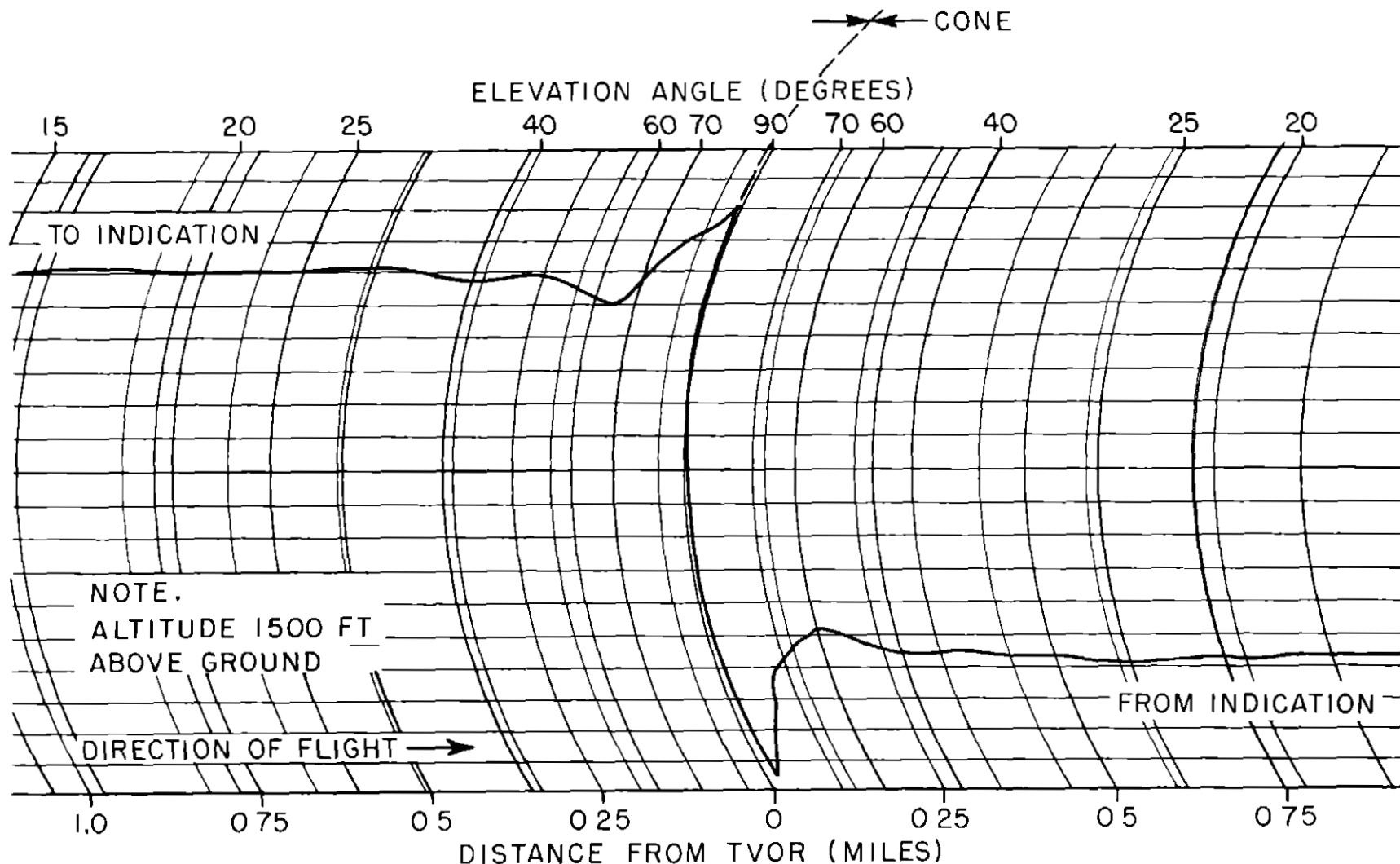


FIG 21 TO-FROM INDICATOR RECORDING OF  
CAA FOUR-LOOP VOR ANTENNA